applied sciences

MDPI

Article

Analysis of Hybrid Ship Machinery System with Proton Exchange Membrane Fuel Cells and Battery Pack

Jure Penga *, Tino Vidović, Gojmir Radica * and Željko Penga

Faculty of Electrical Engineering, Mechanical Engineering and Naval Architecture, University of Split, 21000 Split, Croatia; tino.vidovic.00@fesb.hr (T.V.); zpenga@fesb.hr (Ž.P.)
* Correspondence: jpenga00@fesb.hr (J.P.); goradica@fesb.hr (G.R.)

Featured Application: Repowering of existing vessels with hybrid power system for electricity production and storage with focus on reduced power requirement, increased efficiency, and eliminated greenhouse gas emissions are the applications.

Abstract: As marine traffic is contributing to pollution, and most vessels have predictable routes with repetitive load profiles, to reduce their impact on environment, hybrid systems with proton exchange membrane fuel cells (PEMFC-s) and battery pack are a promising replacement. For this purpose, the new approach takes into consideration an alternative to diesel propulsion with the additional benefit of carbon neutrality and increase of system efficiency. Additionally, in the developed numerical model, control of the PEMFC–battery hybrid energy system with balance of plant is incorporated with repowering existing vessels that have two diesel engines with 300 kWe. The goal of this paper is to develop a numerical model that analyzes and determines an equivalent hybrid ship propulsion system for a known traveling route. The developed numerical model consists of an interconnected system with the PEMFC stack and a battery pack as power sources. The numerical model was developed and optimized to meet the minimal required power demand for a successful route, which has variable loads and sees ships sail daily six times along the same route—in total 54 nautical miles. The results showed that the equivalent hybrid power system consists of a 300 kWe PEMFC stack and battery pack with 424 kWh battery and state of charge varying between 20 and 87%. To power this new hybrid power system, a hydrogen tank of 7200 L holding 284.7 kg at pressure of 700 bar is required, compared to previous system that consumed 1524 kg of diesel and generated 4886 kg of CO_2.

Keywords: proton exchange membrane fuel cell; system modeling; balance of plant; hybrid marine system

Citation: Penga, J.; Vidović, T.; Radica, G.; Penga, Ž. Analysis of Hybrid Ship Machinery System with Proton Exchange Membrane Fuel Cells and Battery Pack. *Appl. Sci.* **2024**, *14*, 2878. https://doi.org/10.3390/app14072878

Academic Editors: José A. Orosa and Francesco Calise

Received: 7 February 2024
Revised: 19 March 2024
Accepted: 27 March 2024
Published: 29 March 2024

1. Introduction

Most countries in the world encourage reductions in harmful emissions [1], which as a consequence causes the price increase of fossil fuels to drive the decrease of greenhouse gas emissions [2], which is an unpopular measure, as fossil fuels are the driving force of marine traffic. From 2008 to 2018, emissions of CO_2 increased by 90%, and predictions are that they will further increase. With IMO regulations for NO_x, CO_2, SO_x, and other emissions becoming more stringent, stakeholders across the board recognize the need for the maritime sector to reduce emissions and decarbonize in order to sustain itself as a business in the future. When a hydrogen fuel cell system is used, the emissions of NO_x, sulfur oxides (SO_x), or PM can be fully eliminated since the fuel cells have no incomplete combustion products, and no pilot fuel is needed [3]. The main measures to reduce consumption and consequently pollution in the shipbuilding industry are to optimize ship engines, propellers, and the hull, which are limiting factors, as the efficiency of each part can only go so far to reach limits of maximal efficiency. To overcome that, a new approach is necessary. The power system generates all power and pollution, and one promising solution is to replace it with a proton exchange membrane fuel cell (PEMFC) in combination with a battery pack. PEMFCs differentiate from internal combustion engines, as they are electrochemical devices for conversion of fuels with hydrogen as an energy carrier to electricity with high efficiency [4]. Other benefits include their generation of completely emission-free energy, their ease of implementation on existing systems that use electricity, and their electrochemical reaction byproduct generation of only pure water and heat. With that said, the PEMFC system is good for long-distance voyages with a constant load and for vessels that travel at relatively short distances with power demand variations, as shown in this paper. Hybrid systems are advantageous in applications where the load is constantly changed, such as the maneuvering of vessels in ports and short distance travel with variable power demand. When a constant load is applied, the PEMFC stack system can be incorporated without the requirement for a high-power battery system; in usage, it can be compared to a diesel system with power demand up to 300 kW. At the moment, diesels outperforms all other systems in towing capability and long-distance range for systems with high output power. A hybrid system that uses a combination of the PEMFC stack and a battery package is very effective and has good dynamic load characteristics, which makes it compatible for replacing the classic marine power systems, like diesel. To analyze and incorporate such a system into vessels for our case, a numerical model was developed. Additionally, this numerical model can be used to simulate different configurations of a hybrid or PEMFC stack system incorporated with other systems that use diesel–electric power (trains or vessels) or any other system that use electricity offshore, off grid, or connected to the grid; it can be scaled, and additional sources of electricity production can be added to give this numerical model offering an even bigger palette of implementation. Corvus Energy developed sustainable marine hydrogen fuel cell systems, which represents a clean and safe alternative power for ships [5]. Petra et al. focused in their study [6] on PEM fuel cells as an energy supply for ships. Their experimental results confirmed that PEM fuel cells are an emission-free solution for electricity generation in ships. The PEM fuel cell was found to be a promising option for marine applications. The main obstacles are the power capacity, cost, and lifetime of the fuel cell assembly [7]. CO_2 emissions are up to 8% lower in the solid oxide fuel cell hybrid system in comparison to a diesel-powered ship during a typical passenger ship voyage [8]. Elkafas A. G. et al. analyzed several issues, such as the new technology and characteristics of different fuel cell systems as well as the international maritime organization rules and policies for hydrogen system applications in the marine industry [9]. In the paper [10], a fuel cell marine power systems model with real-time capabilities was developed and can be implemented for researching performance to obtain an effective system and determining the balance of plant, control, and optimization possibility. To enhance shipping fuel efficiency in an energy management system, optimization for day-ahead power generation plans and dynamically adjusted power splitting were presented in [11]. A hybrid marine propulsion architecture with advanced control strategies can reduce fuel consumption up to 35% while improving noise, maintainability, maneuverability, and comfort [12]. Miotti [13] conducted an analysis of the environmental impact and cost of a proton exchange membrane fuel cell (PEMFC) system for use in fuel cell vehicles in comparison with battery electric and internal combustion engine vehicles. When hydrogen is generated from renewable electricity, fuel cell cars reduce greenhouse gas emissions by 50% compared to gasoline-powered cars. A hybrid marine propulsion system with a heat engine in combination with a battery for electromotors was analyzed in a real load application, and the performance of the components was evaluated [14].

One study proposed and analyzed a hybrid propulsion system for ships that utilizes both the electric energy and thermal energy generated by fuel cells. The proposed hybrid propulsion system can increase energy efficiency by 22.5% [15]. The PEM fuel cell–battery hybrid system was developed and integrated with Li-ion batteries to supply electric power to the waterjet propulsion system of the 20 m tourist boat and successfully operated at

6–8 knots [16]. A hybrid propulsion system consisting of hydrogen wind and solar energy was also analyzed. The results shows that wind power can cover up to 27%, solar power up to 1%, and hydrogen fuel cell up to 100% of the total required power for propulsion [17]. A solid oxide fuel cell (SOFC) for a crude oil tanker was investigated, and the results showed that CO_2 emissions in the SOFC hybrid system were up to 8.8% lower than in the traditional large vessel [8]. A fundamental platform for exploring a hybrid energy system integrated with fuel cell was given in one study, with emphasis on system optimization and energy management strategies [18].

One control strategy of a ship with hybrid power consisting of a 4-stroke diesel generator, solar panels, and battery packs was simulated, and the energy efficiency and emissions were evaluated. The results of the developed hybrid micro-grid system control system showed that it can significantly reduce CO_2 emission and energy cost [19]. From the economic perspective, this system is still expensive. The estimated cost for a fuel cell–battery hybrid propulsion system for repowering a catamaran (20 m long) consisting of (DC) a redundant electric power plant (300 kW) and propulsion system, energy storage system, and marine fuel cell modules is approximately EUR 1,200,000. America's first hydrogen-powered catamaran, Switch Maritime, aims to start operations early next year in San Francisco and is powered with PEMFC-s with 360 kW of power; it has 242 kg of hydrogen storage tanks and a 600 kW electric propulsion system with speed up to 15 knots and cost of USD 10 million. The high cost of hydrogen, safety considerations, and the supply infrastructure are problems for the wide adoption of fuel cell systems [20]. "Handbook for Hydrogen-fueled Vessels", written by DNV and other companies, deals with safety issues for hydrogen as ship fuel [21].

This paper offers detailed insight into the novel hybrid propulsion systems that incorporate a system with a PEMFC stack with battery pack at known load cycles. As the implementation of PEMFC stacks as the energy producer in marine systems is still in its infancy, there is very little literature regarding that field. In this paper, the research focus is on gaining detailed insight into such a system, where the novelty is that PEMFC interacts with the realistic dynamic loading conditions of a vessel in real time, forming a precise and robust carbon-neutral system with higher system efficiency and the same autonomy as a traditional system with diesel engines. An analysis was conducted on a catamaran that was previously in service, and it was considered for refitting from diesel to a PEMFC–battery hybrid propulsion system. The goal was to design an optimal hybrid system that incorporates a PEMFC stack with a battery pack for a known vessel, analyze fuel consumption, and compare it to previous systems with diesel engines, with the additional benefits of silent drive and eliminated pollution compared to previously used internal combustion engines running on diesel fuel. The proposed configuration of the main components for simulation are shown in the methodology chapter. The first goal was to develop a model conceptually and to implement it with methodology and system control using the commercial software AVL CRUISE^{TM} M 2023.1. For implementation of the conceptual model in the software, it was required to connect all parameters, such as vessel kinematics, with the power demand of electric motors and the required electricity consumption from the PEMFC stack and battery system. Additionally, the limitation of discharge on the battery system was set to 20%, with the electric motor rotation speed limitation set to 110 rpm, contrary to the maximum of 370 rpm, until the state of charge reaches 30%.

2. Methodology

The numerical model was conceptually developed as shown in Figure 1 and later implemented in the commercial software AVL CRUISE^{TM} M 2023.1 with a balance of plant system. The conceptual model consists of three main components. the first main component is the PEMFC stack with 300 kWe, and the second is the battery pack with unknown required power that must ensure enough power for the required load profile shown on Table 1. The last component consists of two asynchronous electric motors with a maximum power requirement of 300 kW each (600 kW in total). The required amount of hydrogen with tank capacity is unknown, and simulation was calculated based on the current generated by the fuel cell system.

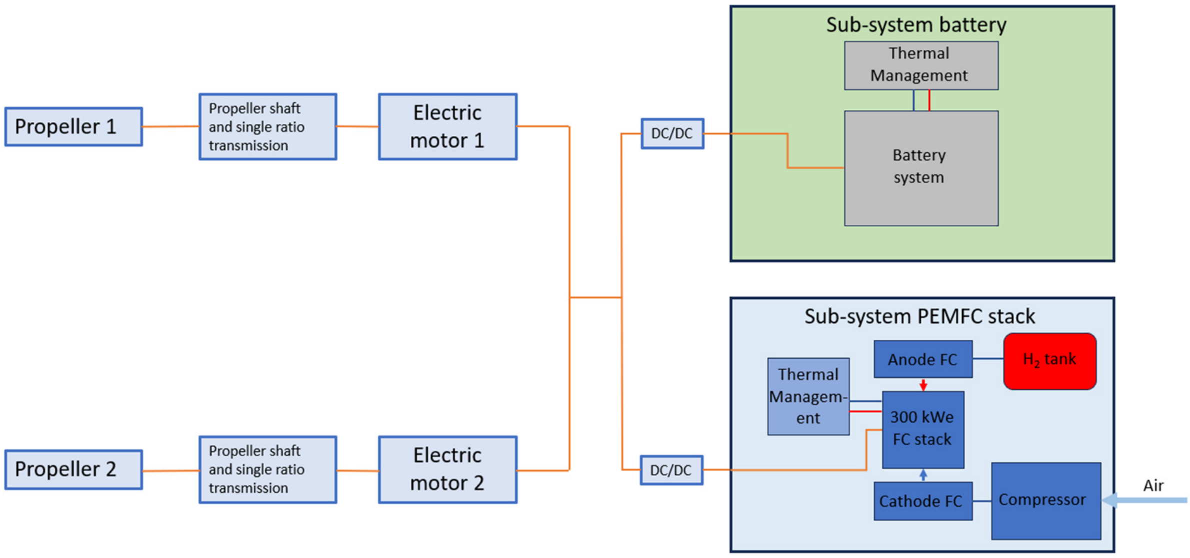

Figure 1. Main components for the numerical model of a hybrid vessel energy system.

Table 1. Voyage route with details of catamaran distance, velocity, time, and required propulsion power for calculation.

Position	Distance	Velocity	Time	Propulsion Power	Distance Crossed
Unit	nm	kts	min	kW	nm
Port of Split—start of route	0	0	3	0	0
Port of Split—starting maneuver	0.5	6	5	100	0.5
Port of Split—sailing ferry to Port Resnik	5.7	12	28.5	600	6.2
Approach maneuver of ferry to Port Resnik	0.3	6	3	80	6.5
Ferry in Port Resnik	0	0	3	0	6.5
Boarding of passengers	0	0	20	0	6.5
Departure of ferry from Port Resnik	0	0	3	0	6.5
Ferry port Resnik—departure maneuver	0.3	6	3	80	6.8
Ferry Port Resnik	5.7	12	28.5	600	12.5
Approaching maneuver to Port of Split	0.5	6	5	80	13
Ferry in Port of Split	0	0	3	0	13
Boarding of passengers	0	0	20	0	13

Additionally, ship resistance was modelled with a longitudinal dynamic model to ensure realistic acceleration and velocity of the vessel; the propeller type is B series, which has a numerical background from the Wageningen B series tests [22]. Torque on the propellers, which generate load on electric motors (EM), ensures a realistic load on the power system.

Balance of plant (BoP) includes the regulation of mass flow rates at the cathode and anode side in the sub-system of the PEMFC, which consists of a compressor at the cathode side with a mass flow of up to 0.3 kg/s and air pumping up to 4 bar from external pressure, which is cooled and circulated through a humidifier before the PEMFC stack to ensure proper humidity for the membrane. Pressure and airflow are controlled via two PID controllers for the compressor and control of the backpressure valve. The power consumption of compressor is defined as linear and dependent on the PEMFC stack load with maximal consumption compared and upscaled from Toyota Mirai PEMFC stack testing [23]. The anode side consists of a large hydrogen tank that stores hydrogen at a pressure of 700 bar and has enough fuel for six voyages; the injection model manages the mixing of hydrogen with water vapor via fuel cell current demand. Recirculation of the unused humid hydrogen is also present, which feeds it back to the system through a Venturi injector, where excess water is removed with a water separator to maintain constant humidity. Pressure is controlled with a PID controller, which controls the Venturi injector's opening. Additionally, to address nitrogen buildup due to crossover through the membrane, a purge valve is periodically opened and releases some of the gas into the surroundings. Some unused hydrogen is lost during the process, but in typical operating conditions, the loss does not exceed 2% of total fuel consumption. Removal of excessive heat is required to maintain a stable temperature of 65 °C in the PEMFC stack, which is managed with a pump that is controlled with PID control and dependent on the load from the PEMFC stack. A pump uses up to 4 kW of electric energy. The active components of the BoP (compressor at the cathode side and pump for thermal management) were simulated as a speed-controlled flange and the corresponding power consumers. This means that the components inside the BoP are controlled indirectly by required current at the PEMFC stack, and required power consumption is calculated with required mass flow rates. As the system consists of the PEMFC stack and battery pack, a power-split strategy was used to take into account the spikes in power demand and insufficient amount of power generated from the PEMFC stack at maximum load in comparison to the pre-defined cyclic load profile with variable loads during the voyage.

3. Numerical Background of Fuel Cell Model

The fuel cell model utilized in this article was designed and extensively examined in [24]. The model is a 0-dimensional electrochemical model that is thermodynamically consistent. It is used to manage the operation of proton exchange membrane fuel cells (PEMFC). Furthermore, the model was also expanded to include the transportation of gases through channels and the gas diffusion layer (GDL), making it quasi-dimensional. The primary characteristic of the model is the simplified form of the Butler–Volmer equation, which clarifies the correlation between voltage and current in an electrochemical cell. The main assumption is a charging transfer coefficient value of 0.5, enabling the utilization of the hyperbolic sine function. Therefore, Equation (2) is derived, which is analogous to the Butler–Volmer equation but considerably easier to handle. The equations are presented below:

$$I_c = I_0^c \cdot \mathrm{e}^{-\frac{E_0^c}{k_B^T}} \left(\widetilde{C}_{O_2}\right)^{0.5} \left(\widetilde{C}_{H_2O}\right) 2\sinh\left(-\frac{e_0 Z_c \eta_c}{k_B T}\right) \tag{1}$$

$$I_0^c = ZF\mathrm{e}^{-\frac{\alpha_c \Delta s_C (T-T^0)}{k_B T}} \mathrm{e}^{-\alpha_c \cdot \ln\left(\frac{k_{RDC}^*}{k_{OXC}}\right)} k_{RDC}^* \tag{2}$$

where I_c is the cathode current, F is the Faraday constant, $\widetilde{C}_{O_2}$ and $\widetilde{C}_{H_2O}$ are the normalized concentrations of oxygen and water, k_B is the Boltzmann constant, Z is the number of electrons in the electrochemical reaction, T is the temperature, k_{RDC}^* and k_{OXC} are the reaction rate constants, e_0 is the elementary charge, and η_C is the reaction kinetics overvoltage on the cathode. Based on Equation (1), it is possible to derive the expression for the overpotential of reaction kinetics, η_C, for the cathode side. However, analogous derivations can also apply to the anode side. This adaptability allows the model to be efficiently implemented in both fuel cell operations and electrolyzer mode.

The single-cell voltage U_{cell} is defined as given:

$$U_{cell} = U_{th} - \eta_c - \eta_a - U_R \tag{3}$$

where U_{th} is the thermodynamic potential, and U_R is voltage ohmic loss.

Ohmic losses are caused by the flow of protons across the membrane, and they have a substantial impact on ionic conductivity. This conductivity is computed using data collected from sources in the literature. Assuming constant ionic conductivity, the ohmic loss increases linearly as the current density increases, which determines the slope of the polarization curve for medium current.

Transport losses refer to the phenomenon of species diffusing through the channels and gas diffusion layer and into the catalyst layer. These losses are quantified using Fick's law of diffusion. These processes define the maximum current densities, namely the current density at which the concentration of the reactant at the catalyst layer begins to decrease. The transport model was modeled with the idea of estimating the concentration of reactants at the catalyst layer ($C_{r_{CL}}$) by multiplying the reactant concentration in the channel ($C_{r_{\mathrm{chan}}}$) by the ratio of the limiting current (I_L) to the current density (I), as expressed by the following equation:

$$C_{r_{CL}} = C_{r_{\mathrm{chan}}} \left(1 - \frac{I}{I_L}\right) \tag{4}$$

$$I_L = ZFSD_{rr} \frac{C_{r_{\mathrm{chan}}}}{\delta_{GDL}} \tag{5}$$

where D_{rr} is diffusion coefficient, and δ_{GDL} is GDL width. The electrochemical model incorporates five calibration parameters, each corresponding to a distinct loss mechanism. Due to the greater significance of activation and transport losses on the cathode side, the parameters for the anode are typically believed to be irrelevant. The membrane material's properties, including density, specific heat capacity, and thermal and ionic conductivity, as well as water diffusion and electro-osmotic drag values are obtained from the literature [25].

Regarding the technical details, the fuel cell model is from the software AVL CRUISE M. In the software, only the dimensions and number of single cells are specified for the stack, and the effective power is calculated according to the available parameter sets (available in the software manual). For the experimental setup, which was not used in this work, it would be required to model the system for 300 kW output power, capable of producing a voltage of 600 V at a current of 500 A. At the moment, high-performance fuel cell stacks are able to produce current densities of 2.0 A/cm^2 with single-cell voltages of 0.6 V. In order to achieve a total current of 500 A, each individual cell should have an active area of at least 250 cm^2. Additionally, the stack should be composed of a minimum of 1000 single cells. To our knowledge, commercial stacks only go up to 250 kW. The dimensions of high-end commercial stacks (e.g., Toyota Mirai, with power output of around 115 kW) have a specific power density of 3.0 kW/dm^3, which would mean that the volume of the fuel cell stack would be at least 100 dm^3.

There are additional approaches for numerical simulation of PEMFC-s, and in CRUISE M, there is simplified model that uses Tafel slope, and the characteristic of the PEMFC stack or single cell is defined as a polarization curve, where it is possible to vary the angle of the curve with coefficients, which makes this simulation zero-dimensional. The most complex numerical approach is with computational fluid dynamics (CFD), with which the PEMFC is considered as a stand-alone system with high complexity, but this requires intensive computation resources and time, so it is useful to define precise parameters in a simplified numerical model, as it can calculate basically any parameter that is required to define the output parameters of heat, current, and voltage production together with consumption of gasses and amount of generated water. One example of CFD simulation for a single-cell PEMFC is given in [26].

4. Developed Numerical Model

In Figure 2, the final model with all components of the system is shown. The first part consists of the PEMFC stack, which was modelled as a quasi-dimensional model with its numerical background explained in the previous chapter. An equivalent circuit model for the battery pack was used, and the model consists of a controlled voltage source with Ohmic resistance, which is used to describe instantaneous voltage response to current input. Additionally, a thermal model called "a solid wall" was implemented to predict the transient thermal behavior of the battery. Moreover, multiple battery elements were connected via electrical pins to construct an electrical network acting as a battery module or battery pack. Open-circuit voltage is defined for classic Li-ion batteries [27], as in Figure 3. Ohmic resistance was taken at the temperature of 25 °C and defined as in Figure 4.

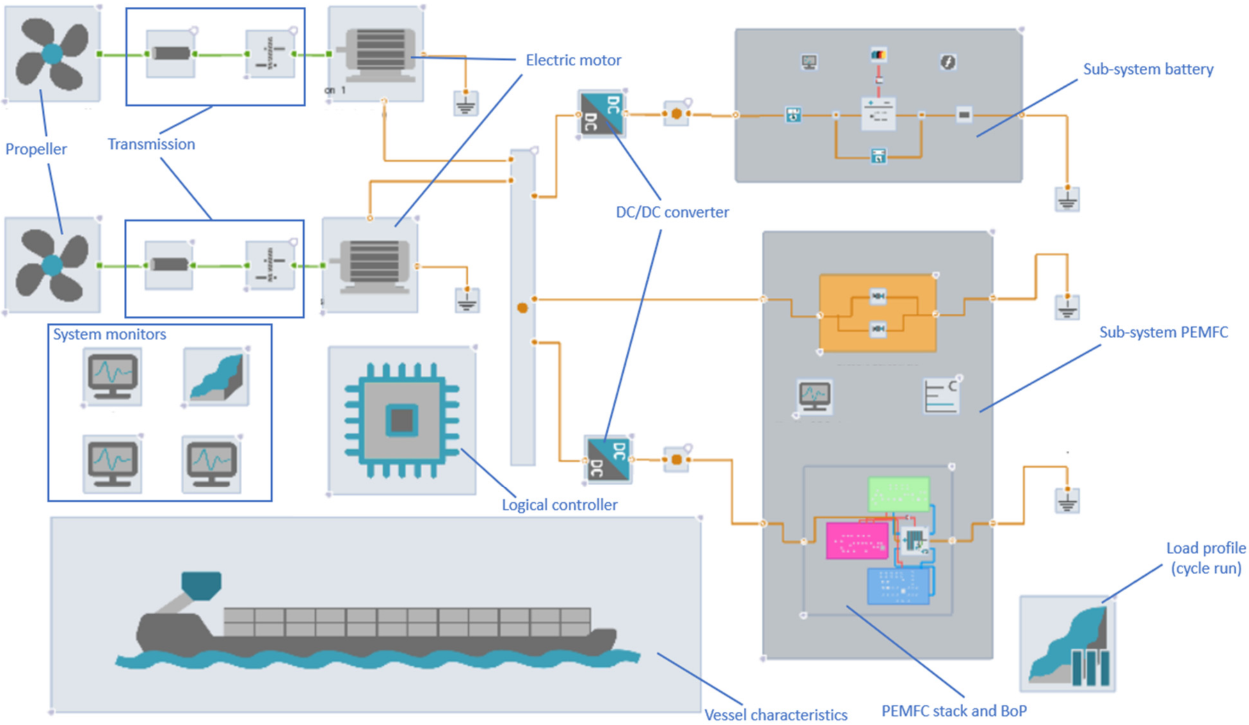

Figure 2. Main components of developed numerical model in AVL CRUISE^{TM} M 2023.1.

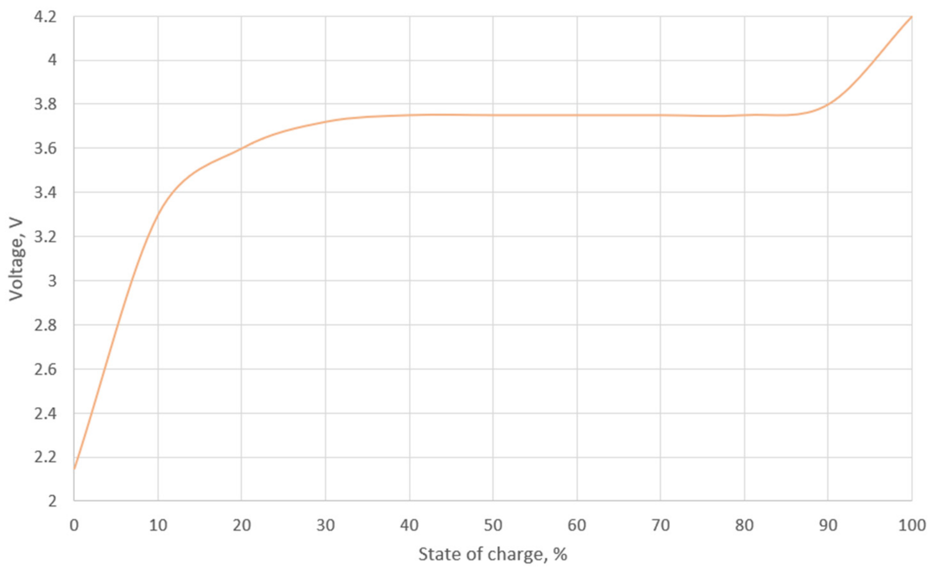

Figure 3. Voltage distribution of battery pack for different states of charge.

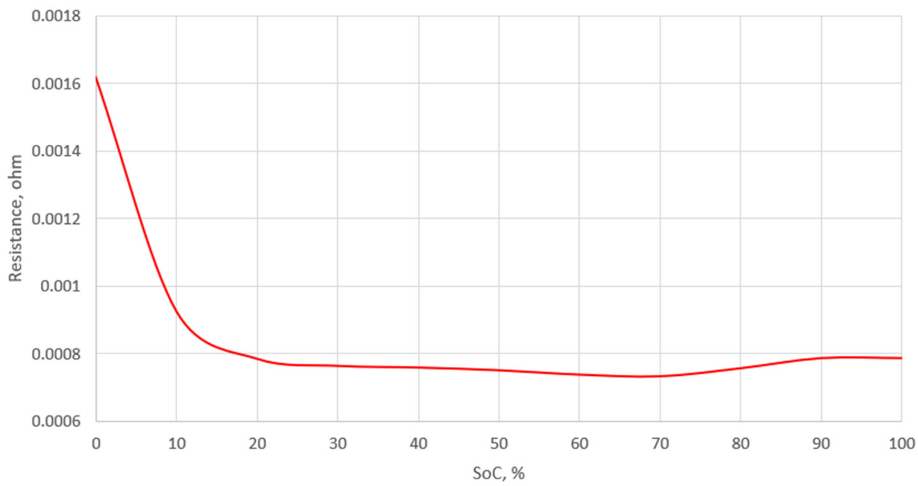

Figure 4. Ohmic resistance distribution of battery pack for different states of charge.

Additionally, the maximal current of charging is defined for a given SoC, which is shown in Figure 5, where the maximal charging current of the battery system is shown with a blue line, and the maximal current of the PEMFC stack is shown with an orange line (500 A).

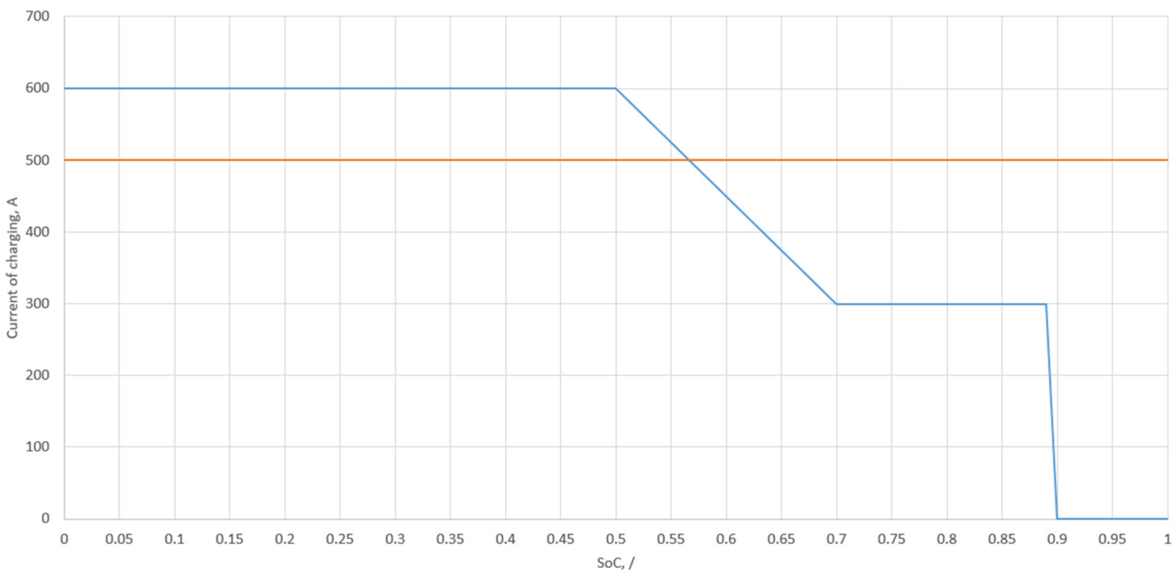

Figure 5. Maximal speed of charging for battery system dependent on SoC.

Many combinations of battery packages have been implemented, and the optimal battery package configuration consists of 110 battery packages connected in parallel with 130 batteries connected in series (total 14,300 batteries), with each battery having a voltage range from 2.5 to 4.2 V, where nominal voltage is 3.7 V, and a capacity of 8 Ah. Discharge voltage is defined as in Figure 3. The total calculated combined power of the battery pack is 424 kWh with state of charge (SoC) at 100%. Ohmic losses between each battery for this simulation were neglected, as the main goal was to examine the required power from auxiliary storage to satisfy the required condition.

There are two electric motors (EM-s) that are the same, defined as asynchronous engines, with a demanded maximum power of 300 kW each or 600 kW in total. They have a defined torque for rotation speed, which is shown in Figure 6 for a full spectrum of load. For this simulation, the spectrum of load has constant torque, as it is from 0 to 370 rpm.

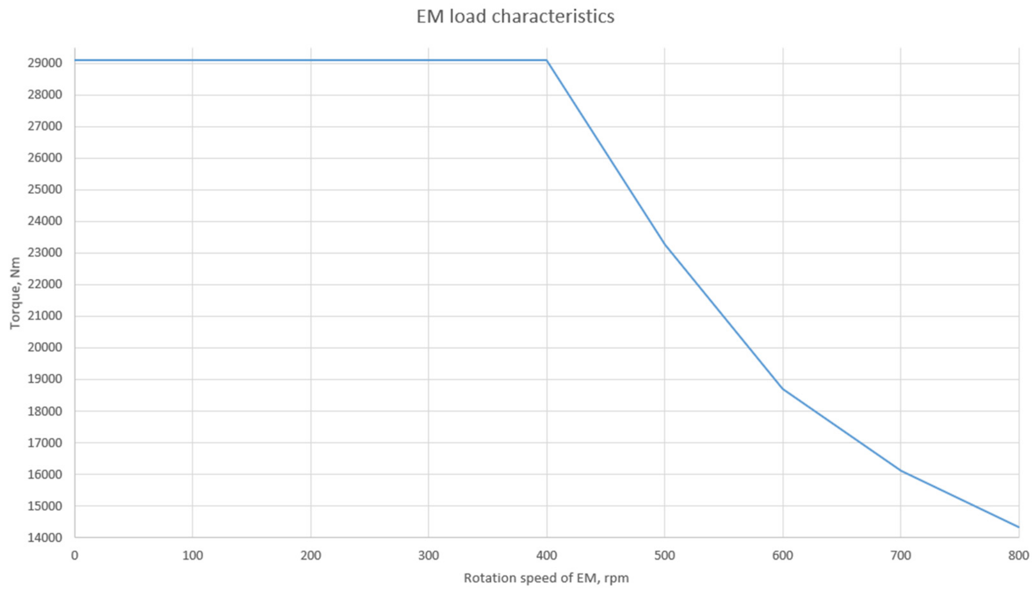

Figure 6. Torque distribution of electric engine per number of revolutions in one minute.

Propellers that are connected to EM-s are defined as classic B series propellers by [22], with a diameter of 1.5 m, four blades, a pitch to diameter ratio of 1.2, and a disk area coefficient of 0.7. While on full load advance, the coefficient is 0.73.

The marine vessel model, which is powered by a fuel cell and a battery, is a sophisticated system with multiple interlinked components. The vessel was modeled as a longitudinal dynamic model and designed to calculate various key parameters related to a vessel's forward and backward movement. Initially, the model defined parameters such as the ship's mass (80 t), thrust force, external forces, resistance force, initial speed, and thrust deduction factor. With those parameters, the numerical model could calculate ship acceleration with consideration of the net forces acting on it, including both the thrust and resistance forces, then dividing them by the ship's mass. The ship's velocity was then updated by integrating acceleration over time, starting from an initial velocity value. Furthermore, the position of the ship is determined by integrating velocity over time. The ship's resistance was determined from experimentally validated results.

The propeller speed demand was determined by load profile, which simulates an average cyclical navigation route of 13 nautical miles with the load profile presented by the values in Table 1, which are graphically shown in Figure 7.

The actual propeller speed is regulated with a PID controller, which maintains the desired propeller speed with adjustments of the EM load based on the comparison between the actual and desired speeds.

In terms of energy storage and management, the system includes a battery pack that acts as energy storage, supplying the excess power demand that cannot be met by the fuel cell to the EM and other components that require electricity. The PEMFC stack is the only source of electricity for battery charging with conversion of chemical energy from hydrogen to electrical energy.

Significant aspects of the system include power demand and voltage regulation. The controller function calculates the total power required for the EM, compressor, steering pump, and battery charging. Based on this power demand and the battery's SoC, the controller decides the PEMFC stack's power output. If the power demand is high and the battery's SoC low, PEMFC operates at its nominal power, utilizing the hysteresis mechanism to avoid frequent on–off cycling under certain conditions. The hysteresis mechanism has a boundary condition to limit propeller speed to 110 rpm if the SoC drops below 20%, and it holds that limit until the SoC reaches 30%. The controller also determines the fuel cell's current demand considering the voltage limits and whether the fuel cell is on or off. It includes a delay feature to simulate the gradual ramping up of current when the fuel cell activates, and a low-pass filter is applied to smooth out any spikes in the output current. Finally, the necessary current from the PEMFC was determined by dividing the calculated power demand by the system voltage. Additionally, stable voltage across the system is maintained by two DC/DC controllers, ensuring efficient and consistent power supply.

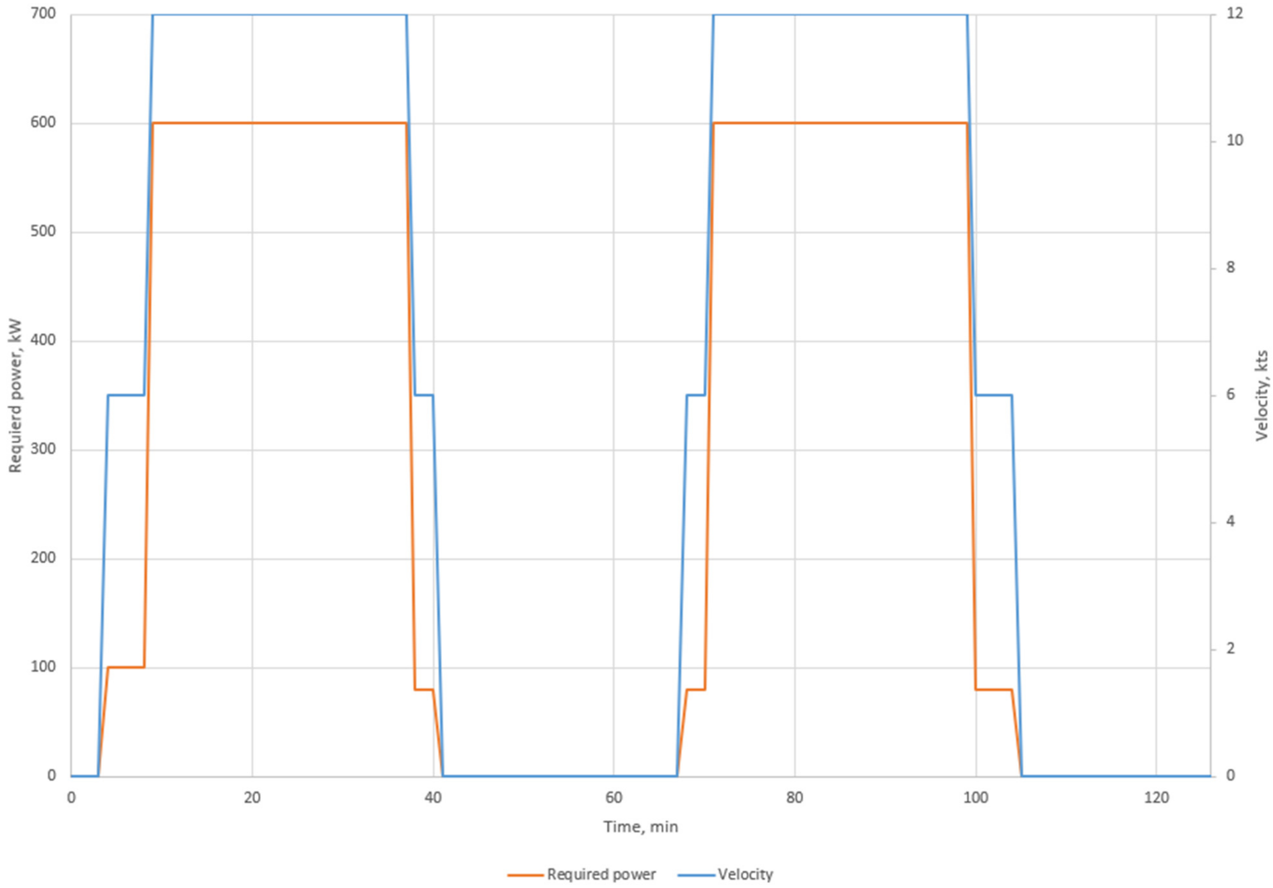

Figure 7. Velocity and required propulsion power for duration of one voyage.

5. Results and Discussion

In Figure 8, the SoC, total resistance of vessel, and PEMFC power are shown for six voyages, where all components within the system respond to each other with the hysteresis mechanism implemented for the PEMFC stack, but for this configuration, it was not activated. This is better displayed in Figure 9, which has same parameters as in Figure 8 but is given for only one voyage, where it is seen that total resistance follows the pattern defined on Table 1, with additional time between recharging of the battery and repeating the voyage. It can be seen that the SoC and PEMFC power tracked the ship resistance, as the PEMFC used the battery system for compensation while getting to the work load, and when the load reached the required 600 kW, battery system started to discharge; after the first part of trip (Port of Split to Port of Resnik), the PEMFC continued to work on maximum load until the battery system reached the required SoC, as shown in Figure 5. To show the hysteresis mechanism there was a simulation of one cycle of the battery pack of 100 battery packages connected in parallel with 100 batteries connected in series (total 10,000 batteries) with a total power of 296 kWh; results are shown in Figure 10, with the hysteresis mechanism activated after the 89th minute and kept until the end of the route. As a consequence. the total distance passed changed from 13.8 nm to 11.6 nm.

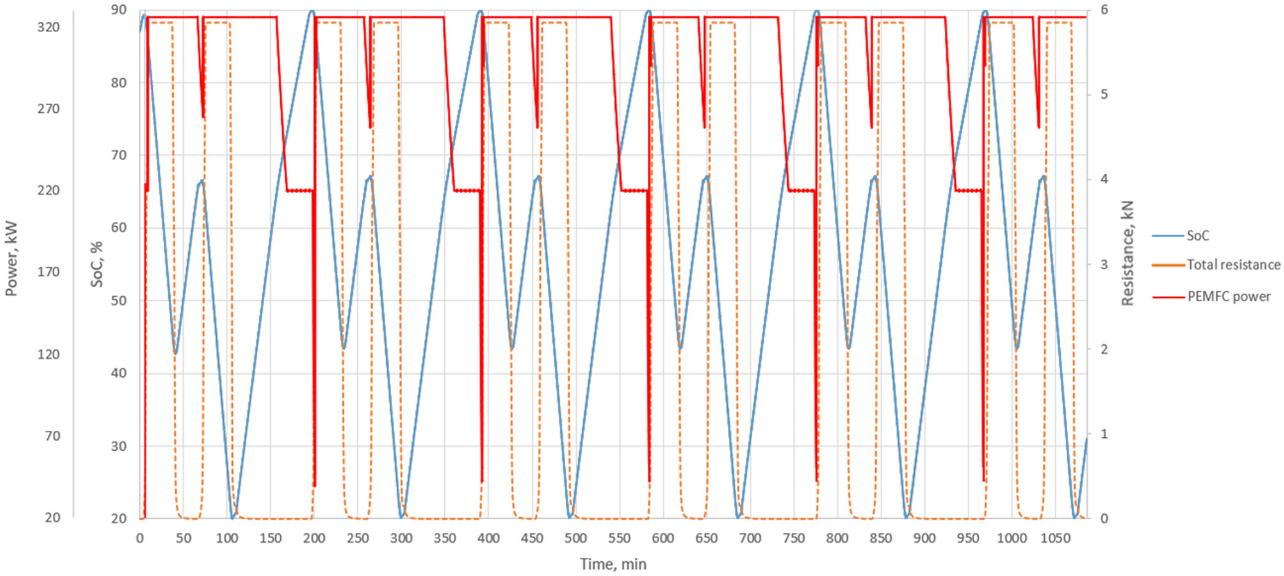

Figure 8. Comparison of power, SoC, and total ship resistance for six voyages.

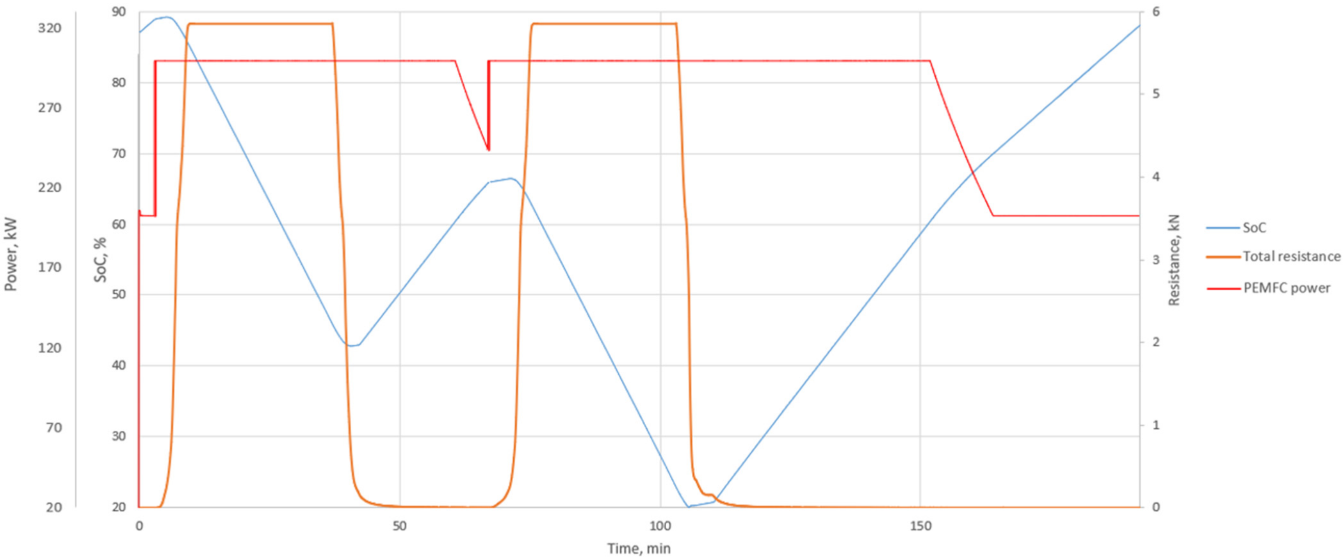

Figure 9. Comparison of power, SoC, and total ship resistance for one voyage.

The results in Figures 8 and 9 show that the system with the PEMFC stack of 300 kWe and battery pack with 424 kWh with an initial SoC of 87% at the start of the voyage can replace the previous configuration of two diesel engines with an output power of 300 kW each and meet all required demands for this route. With the required velocity and duration of voyage shown in Figure 8, the SoC increased to 88.14%, which ensures that route is repeatable, as the final SoC is higher than the initial one. Total consumption for one voyage was 47.45 kg, and for six voyages with the PEMFC as only source of power, it was 284.7 kg of hydrogen in comparison to diesel engines, which require 254 kg for one voyage and 1524 kg of diesel for six voyages. Fuel consumption of the hybrid system can be reduced on the last voyage by 14.6 kg, as it is end of the day, so the battery pack can be recharged with an outer electric energy supply. For 284.7 kg of hydrogen, the storage capacity required is 7200 L under a pressure of 700 bar. All greenhouse gases, including CO_2, are removed in comparison to the 4886 kg of CO_2 generated from diesel engines, which was calculated from the IMO Resolution MEPC.308(73) [28].

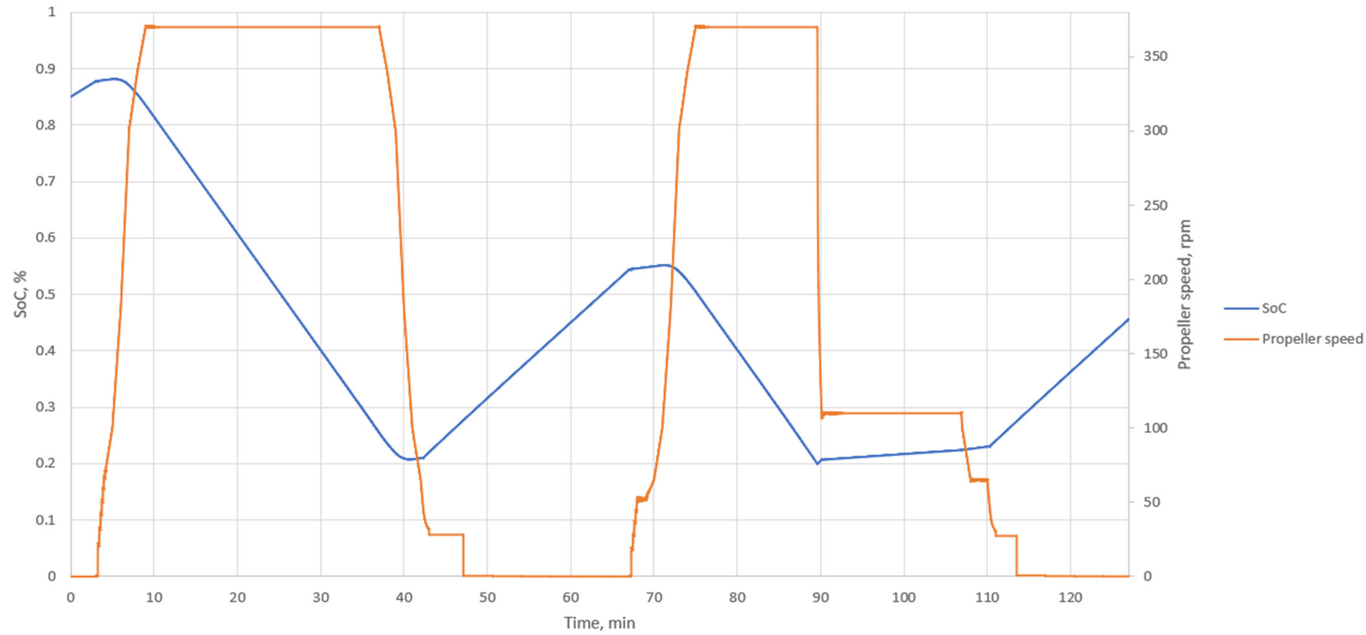

Figure 10. SoC and propeller speed for reduced size of battery package and activated hysteresis mechanism.

If the time that the ship is moored in the harbor increases, the battery pack capacity could be reduced, and approximately 2 more minutes in full load increases the total consumption of energy up to 3.5% with the increase of distance traveled from 13 nm to 13.8 nm per voyage. In conclusion, this means that the realistic power consumption is smaller than in the numerical model. As the system is 100% electric and compatible with a conventional electric energy grid, it is possible to implement the system with photovoltaics and plug-in charge of batteries, which will consequently significantly reduce the required battery pack power, or it is possible to implement another PEMFC stack as an auxiliary or upscaled power system to meet electric energy requirements.

6. Conclusions

The research has shown repowering an existing vessel with a PEMFC–battery hybrid power system increased efficiency and eliminated greenhouse gas emissions compared to the previously installed diesel propulsion system. The new numerical model of the hybrid power system was developed and can be used for different hybrid systems and power demand optimization and as a very flexible system for implementation in any electric-dependent power facility with different applications. The model will be further developed for BoP optimization in realistic cycles of operation. For further development of the numerical model, an intended improvement would be a system with different output power of the PEMFC stack or a combination of one main and another auxiliary PEMFC stack and the implementation of photovoltaics with detailed insight into their power production and potential to additionally reduce the requirement for batteries and increase possibilities for the implementation of this numerical model. Results have shown that the system using the PEMFC stack with battery system requires a significantly smaller amount of fuel, namely 18.68% of fuel by mass in comparison to the previous system (284.7 kg of hydrogen in comparison to 1524 kg of diesel), which is emission-free and offers high flexibility for further system upgrades, as such a system generates electricity, and additional components can be added without the necessity of additional complex refitting. The total efficiency of the PEMFC system is around 60% [29] in comparison to diesel engines that have a maximal efficiency around 45% for systems with similar power.

There are many ways to further improve this system with additional implementation of an auxiliary PEMFC stack, with which the required power of batteries would be reduced, such as photovoltaic (PV) collectors for electricity production, as this vessel has a large unused area on deck, and the area of the voyage has very good conditions for such energy production. This system would have the potential for generation of around 48 kWp of electricity, as the deck area is around 240 m^2 (about 5 m^2 for 1 kWp), which would dramatically reduce electricity consumption from the batteries during the voyage and improve charging speed, as the maximum current of charging is 600 A, and there is 100 A deficiency of charging, as the PEMFC stack has a maximal current of 500 A. Additionally, the implementation of charging from the grid in port would significantly reduce consumption of hydrogen (around 87.48 kg), as the load of the PEMFC stack during the time in port can be removed, and the speed of charging can be set to 600 A.

Author Contributions: Conceptualization, J.P. and T.V.; data curation, J.P., T.V. and G.R.; formal analysis, J.P. and T.V.; funding acquisition, G.R.; investigation, J.P., T.V. and G.R.; methodology, J.P., T.V., G.R. and Ž.P.; project administration, G.R. and Ž.P.; software, J.P. and T.V.; supervision, G.R. and Ž.P.; validation, J.P., T.V., G.R. and Ž.P.; visualization, J.P. and T.V.; writing—original draft, J.P. and T.V.; writing—review and editing, J.P., T.V., G.R. and Ž.P. All authors have read and agreed to the published version of the manuscript.

Funding: This work has been fully supported by the Croatian Science Foundation under the project IP.2020-02-6249.

Institutional Review Board Statement: Not applicable.

Informed Consent Statement: Not applicable.

Data Availability Statement: The data presented in this study are available in article.

Conflicts of Interest: The authors declare no conflicts of interest.

References

1. Vidović, T.; Šimunović, J.; Radica, G.; Penga, Ž. Systematic Overview of Newly Available Technologies in the Green Maritime Sector. *Energies* **2023**, *16*, 641. [CrossRef]
2. Adamolekun, G. Carbon price and firm greenhouse gas emissions. *J. Environ. Manag.* **2024**, *349*, 119496. [CrossRef] [PubMed]
3. Fourth IMO GHG Study 2020 Full Report. Available online: https://www.imo.org/en/ourwork/Environment/Pages/Fourth-IMO-Greenhouse-Gas-Study-2020.aspx (accessed on 12 December 2023).
4. Vidović, T.; Tolj, I.; Radica, G.; Ćoko, N.B. Proton-exchange membrane fuel cell balance of plant and per-2 formance simulation for vehicle applications. *Int. J. Environ. Res. Public Health* **2022**, *15*, 8110. [CrossRef]
5. Marine Power with Toyota Fuel Cell Technology. Available online: https://www.toyota-europe.com/news/2023/marine-power (accessed on 12 December 2023).
6. Pietra, A.; Gianni, M.; Zuliani, N.; Malabotti, S.; Taccani, R. Experimental characterization of a PEM fuel cell for marine power generation. In *E3S Web of Conferences*; EDP Sciences: Paris, France, 2022. [CrossRef]
7. Xing, H.; Stuart, C.; Spence, S.; Chen, H. Fuel cell power systems for maritime applications: Progress and perspectives. *Sustainability* **2021**, *13*, 1213. [CrossRef]
8. Lee, J.I.; Yoon, B.Y.; Cha, S.W. Analysis of solid oxide fuel cell hybrid power system in marine application for CO_2 reduction. *Energy Rep.* **2023**, *9*, 3072–3081. [CrossRef]
9. Elkafas, A.G.; Rivarolo, M.; Gadducci, E.; Magistri, L.; Massardo, A.F. Fuel Cell Systems for Maritime: A Review of Research Development, Commercial Products, Applications, and Perspectives. *Processes* **2023**, *11*, 97. [CrossRef]
10. Bagherabadi, K.M.; Skjong, S.; Bruinsma, J.; Pedersen, E. System-level modeling of marine power plant with PEMFC system and battery. *Int. J. Nav. Archit. Ocean. Eng.* **2022**, *14*, 100487. [CrossRef]
11. Xie, P.; Asgharian, H.; Guerrero, J.M.; Vasquez, J.C.; Araya, S.S.; Liso, V. A two-layer energy management system for a hybrid electrical passenger ship with multi-PEM fuel cell stack. *Int. J. Hydrogen Energy* **2024**, *50*, 1005–1019. [CrossRef]
12. Geertsma, R.D.; Negenborn, R.R.; Visser, K.; Hopman, J.J. Design and control of hybrid power and propulsion systems for smart ships: A review of developments. *Appl. Energy* **2017**, *194*, 30–54. [CrossRef]
13. Miotti, M.; Hofer, J.; Bauer, C. Integrated environmental and economic assessment of current and future fuel cell vehicles. *Int. J. Life Cycle Assess.* **2017**, *22*, 94–110. [CrossRef]
14. Barelli, L.; Bidini, G.; Gallorini, F.; Iantorno, F.; Pane, N.; Ottaviano, P.A.; Trombetti, L. Dynamic modeling of a hybrid propulsion system for tourist boat. *Energies* **2018**, *11*, 2592. [CrossRef]
15. Oh, D.; Cho, D.-S.; Kim, T.-W. Design and evaluation of hybrid propulsion ship powered by fuel cell and bottoming cycle. *Int. J. Hydrogen Energy* **2023**, *48*, 8273–8285. [CrossRef]

16. Choi, C.H.; Yu, S.; Han, I.-S.; Kho, B.-K.; Kang, D.-G.; Lee, H.Y.; Seo, M.-S.; Kong, J.-W.; Kim, G.; Ahn, J.-W.; et al. Development and demonstration of PEM fuel-cell-battery hybrid system for propulsion of tourist boat. *Int. J. Hydrogen Energy* **2016**, *41*, 3591–3599. [CrossRef]
17. Dolatabadi, S.H.; Ölçer, A.I.; Vakili, S. The Application of Hybrid Energy system (Hydrogen Fuel cell, wind, and solar) in shipping. *Renew. Energy Focus* **2023**, *46*, 197–206. [CrossRef]
18. Bukar, A.L.; Tan, C.W. A review on stand-alone photovoltaic-wind energy system with fuel cell: System optimization and energy management strategy. *J. Clean. Prod.* **2019**, *221*, 73–88. [CrossRef]
19. Yu, W.; Zhou, P.; Wang, H. Evaluation on the energy efficiency and emissions reduction of a short-route hybrid sightseeing ship. *Ocean. Eng.* **2018**, *162*, 34–42. [CrossRef]
20. Waseem, M.; Amir, M.; Lakshmi, G.S.; Harivardhagini, S.; Ahmad, M. Fuel cell-based hybrid electric vehicles: An integrated review of current status, key challenges, recommended policies, and future prospects. *Green Energy Intell. Transp.* **2023**, *2*, 100121. [CrossRef]
21. Handbook for Hydrogen-Fuelled Vessels. Available online: https://www.dnv.com/maritime/publications/handbook-for-hydrogen-fuelled-vessels-download/ (accessed on 12 December 2023).
22. Bernitsas, M.M.; Ray, D.; Kinley, P. KT, KQ and Efficiency Curves for the Wageningen B-Series Propellers. Available online: https://deepblue.lib.umich.edu/bitstream/handle/2027.42/91702/Publication_No_237.pdf?sequence=1&isAllowed=y (accessed on 31 January 2024).
23. Lohse-Busch, H.; Stutenberg, K.; Duoba, M.; Liu, X.; Elgowainy, A.; Wang, M.; Wallner, T.; Richard, B.; Christenson, M. Automotive fuel cell stack and system efficiency and fuel consumption based on vehicle testing on a chassis dynamometer at minus 18 °C to positive 35 °C temperatures. *Int. J. Hydrogen Energy* **2020**, *45*, 861–872. [CrossRef]
24. Kravos, A.; Ritzberger, D.; Tavc, G.; Hametner, C.; Jakubek, S.; Katras, T. Thermodynamically consistent reduced dimensionality electrochemical model for proton exchange membrane fuel cell performance modelling and control. *J. Power Sources* **2020**, *454*, 227930. [CrossRef]
25. Springer, T.E.; Wilson, M.S.; Gottesfeld, S. Modeling and Experimental Diagnostics in Polymer Electrolyte Fuel Cells. *J. Electrochem. Soc.* **1993**, *140*, 3513–3526. [CrossRef]
26. Penga, J.; Radica, G.; Penga, Ž.; Xing, L.; Bonković, K.; Xu, Q. Optimization of auxiliary channel dimensions for improved water removal from PEM fuel cells. In Proceedings of the 8th International Conference on Smart and Sustainable Technologies SpliTech 2023, Bol, Croatia, 20–23 June 2023.
27. Li-Ion Voltage Analysis. Available online: https://siliconlightworks.com/li-ion-voltage (accessed on 12 December 2023).
28. International Maritime Organization. *Guidelines on the Method of Calculation of the Attained Energy Efficiency Design Index (Eedi) for New Ships*; International Maritime Organization: London, UK, 2022.
29. Technology Assessment of a Fuel Cell Vehicle: 2017 Toyota Mirai Energy Systems Division. Available online: www.anl.gov (accessed on 12 December 2023).